

Process-induced crystallite size and dissolution changes elucidated by a variety of analytical methods

Guillermo Torrado ^a, Susana Fraile ^b, Susana Torrado ^b, Santiago Torrado ^{b,*}

^a *Departamento de Farmacia y Tecnología Farmacéutica, Facultad de Farmacia, Universidad de Alcalá de Henares, Madrid, Spain*

^b *Departamento de Farmacia y Tecnología Farmacéutica, Facultad de Farmacia, Universidad Complutense de Madrid, Madrid 28040, Spain*

Received 9 September 1997; received in revised form 15 December 1997; accepted 18 December 1997

Abstract

The purpose of this work was the study, by multiple analytical techniques, of the physico-chemical changes and the dissolution behaviour of various recrystallized forms obtained through different recrystallization methods. Scanning electron microscopy, differential scanning calorimetry, powder X-ray diffraction and infra-red spectroscopy were applied to evaluate the samples. These analytical techniques showed changes in particle morphology, and ruled out the possibility of the existence of polymorphs, pseudopolymorphs, totally amorphous forms or chemical structural changes. The powder X-ray diffraction technique showed great reductions in the drug crystallite sizes induced by both recrystallization methods. The decreased drug crystallite sizes can explain the faster dissolution rates of the recrystallized samples as compared to the non-recrystallized drug acetylsalicylic acid (ASA), or to the physical mixtures of drug (ASA) and carrier (mannitol). © 1998 Elsevier Science B.V. All rights reserved.

Keywords: Recrystallization; Crystallite size; Scanning electron microscopy; Differential scanning calorimetry; Powder X-ray diffraction; Infra-red spectroscopy; Drug dissolution

1. Introduction

Dissolution rate depends on several factors, one of which is the particle size. A reduction in particle size generally increases the dissolution rate. On the other hand, during the recrystallization pro-

cess, changes in the crystal size or crystalline disorder may appear and these changes could have significant consequences with respect to dissolution rate.

Changes in the physical state of raw material occurring as a result of particle size reduction are well documented (Buckton et al., 1988; Ghosh et al., 1995). Recently, more subtle changes in the

* Corresponding author.

physical state have been observed during the recrystallization process (Shively and Myers, 1993; Ward and Schultz, 1995). For some pharmaceutical drugs, a low degree of crystallinity decreases stability (Duddu and Weller, 1996). The formation of polymorphs or changes in solvation are examples of gross alterations in powder states and have been observed in many drugs (Caira et al., 1995; Ghosh et al., 1995; Jozwiakowski et al., 1996).

Freeze-drying is particularly useful for the study of crystalline and amorphous physical forms of different drugs (Grocker and McCauley, 1995; Saleki-Gerhardt et al., 1995). Likewise, spray-drying and rotary evaporation are techniques used for obtaining solid dispersions and in the recrystallization process (Otsuka et al., 1993).

It is possible to observe the appearance of microcrystalline forms by some freeze-drying processes. These solid state forms are characterized by their low crystallinity percentages evaluated with an X-ray diffraction technique. However, these forms show differential scanning calorimetry (DSC) endothermic melting peaks characteristic of crystalline forms (Shively and Myers, 1993; Ward and Schultz, 1995).

The aim of this work is the study of the crystalline forms obtained through different recrystallization methods by multiple analytical techniques. ASA (acetylsalicylic acid) was selected as a raw material because it has no polymorphs or solvated forms and it is thus possible to study the correlation between the crystallization patterns observed and the dissolution profiles of ASA recrystallized by these processes.

2. Materials and methods

2.1. Materials

ASA USP 25 (Merck, Darmstadt, Germany) with a selected particle size of 0.3–0.2 mm and mannitol NF (ICI Americas Inc., USA) with a selected particle size of 0.3–0.2 mm were used. All other ingredients were of reagent grade or better (Merck, Darmstadt, Germany).

2.2. Methods

2.2.1. Powder samples

2.2.1.1. Physical mixtures. Non-recrystallized physical mixtures of ASA and mannitol (ratios 4:0, 3:1, 1:1 and 1:3) were sieved and fractions of between 0.3–0.2 mm were isolated for each ratio and used as pattern with regard to the data obtained from the different analytical methods.

2.2.1.2. Recrystallized powders. Initial mixed powders of ASA and mannitol at various ratios (4:0, 3:1, 1:1 and 1:3) were dissolved in 500 ml of ethanol:water (1:1) solution. ASA content was 30 g for each formulation. The recrystallization was obtained by two different methods as follows.

For method I the different solutions were fed into a mini-spray drier (Büchi B-191, Flawil, Switzerland) through a peristaltic pump at 1.5 ml/min. The temperature at the inlet of the drying chamber was maintained at 80°C.

For method II the different solutions were dried by rotary evaporation (Büchi System, Flawil, Switzerland) under reduced pressure at a constant temperature of 80°C.

The different recrystallized powders of ASA and mannitol at various ratios obtained with methods I and II were sieved and fractions between 0.3 and 0.2 mm were isolated. So the recrystallized forms studied were I-(4:0), I-(3:1), I-(1:1), I-(1:3), II-(4:0), II-(3:1), II-(1:1), and II-(1:3).

2.2.2. Scanning electron microscopy (SEM)

Particle morphology, size and shape were analyzed by scanning electron microscopy (SEM) on a Jeol 6400 electron microscope. All micrographs were the product of secondary electron imaging used for surface morphology identification at 500 × magnification.

2.2.3. Infra-red spectroscopy

A Perkin Elmer FT-IR Paragon 1000 infra-red spectrometer was used. The scan range was 500–4000 cm^{-1} . Each spectrum was automatically averaged over 16 scans obtained at a spectral resolution of 4 cm^{-1} . A sample cup filled with

dried KBr powder was used as the background data set.

2.2.4. Differential scanning calorimetry

For differential scanning calorimetry (DSC), samples of 2–6 mg in loosely covered aluminium pans were heated from 50 to 250°C at the rate of 10°C/min under nitrogen purge, with an empty, loosely covered aluminium pan as the reference, in a differential scanning calorimeter DSC Mettler TA 8000.

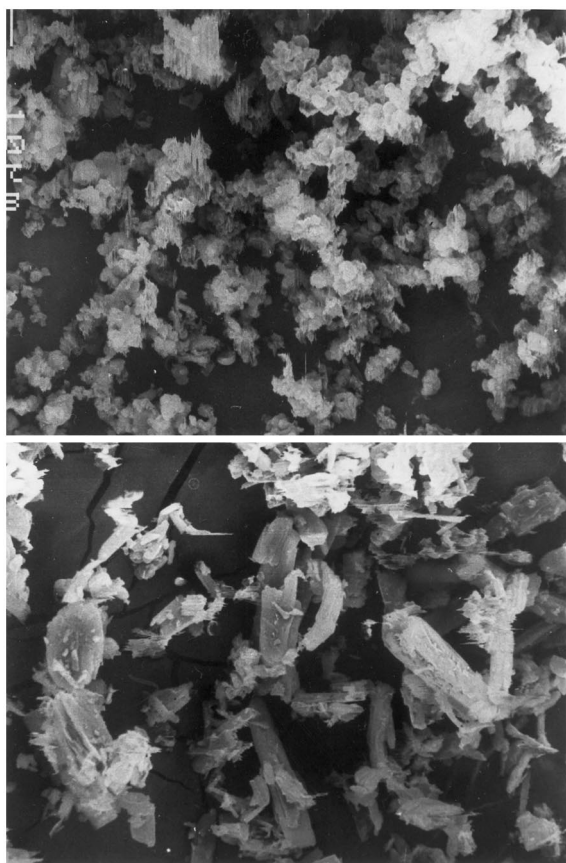


Fig. 1. Scanning electron micrographs of acetylsalicylic acid:mannitol. Top figure represents the spray-dried recrystallized form I-(3:1) and the bottom figure represents the rotary recrystallized form II-(3:1). Photographs taken at a magnification of 500 ×.

2.2.5. Powder X-ray diffraction: structural and crystal size characterization

The structural characterization of the material included conventional θ -2 θ powder X-ray diffraction (Philips X'Pert-MPD) (CAI Difracción rayos X, Farmacia, UCM) of all samples under study. Measurements were carried out with 2 θ 5–40°, using a step size of 0.04° (2 θ) and 1-s time per step.

Two peaks at 7.857° and 15.857° (2 θ), with a (hkl) reflection of 100 and 002 respectively, were used to estimate the ASA crystallite sizes. The instrumental broadening was determined using an ASA standard which has a crystallite size bigger than 1 μ m.

A profile fitting based on Marquardt non-linear least squares algorithm (Schreiner and Jenkins, 1983) was subsequently applied to selected ranges of the data, allowing the elimination of background contributions and the separation of overlapping diffraction maxima. The values of diffracted intensity and full width at half maximum (FWHM) for each peak are taken from the fitted profiles to estimate the average crystallite size by means of Scherrer's equation:

$$\text{Average crystallite size} = \frac{K\lambda}{\beta \cos \theta}$$

Where β is the difference in FWHM between broadened and standard maxima.

The arithmetical mean of the two average crystallite sizes obtained with the two peaks selected, gave us the crystallite size of the different recrystallized forms.

2.2.6. In vitro drug release

For drug release testing, the USP 23 (1995) apparatus I (Turu-Grau) with a rotation speed of 50 rpm, was used. The dissolution medium was 500 ml of pH 4.5 acetate buffer. Samples were analyzed in a Beckman DU-6 spectrophotometer at 265 nm. The studies were repeated three times to obtain the mean value. With these data the $\text{MDT}^{\text{vitro}}$ (mean dissolution time) of the different recrystallized forms was calculated (Torrado et al., 1996a).

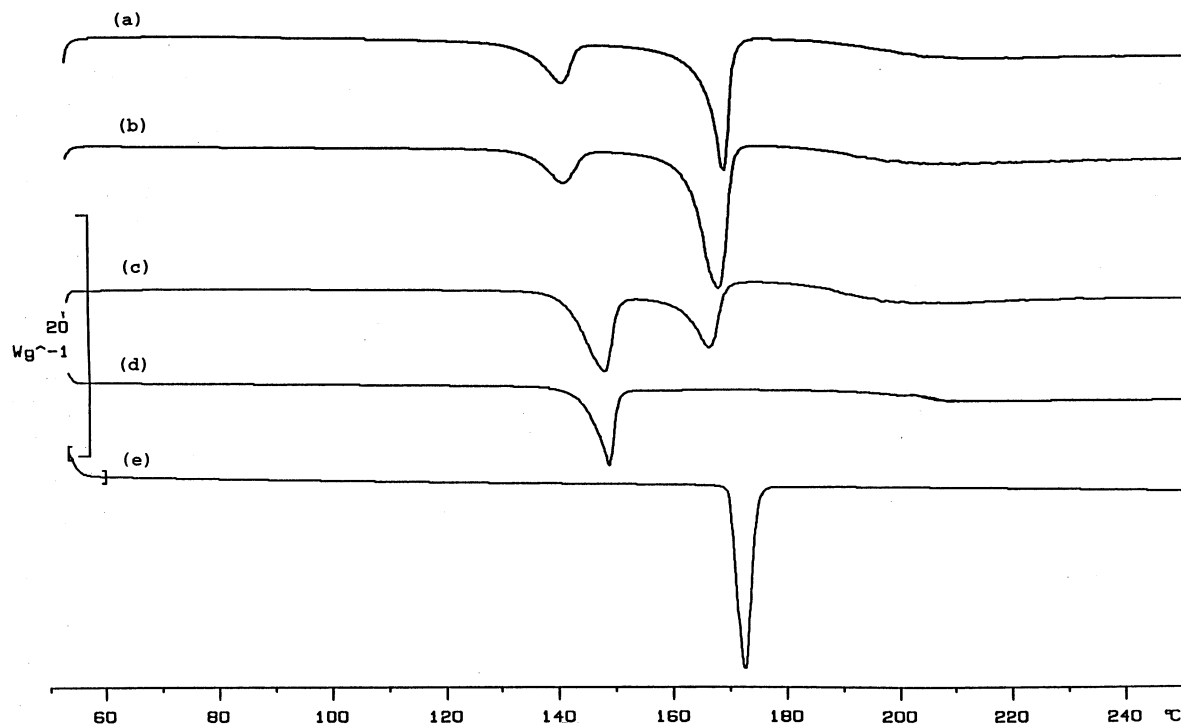


Fig. 2. Differential scanning calorimetry scans of: (a) rotary evaporation recrystallized form II-(1:1); (b) spray-drier recrystallized form I-(1:1); (c) non-recrystallized physical mixtures of ASA and mannitol (1:1); (d) acetylsalicylic acid; and (e) mannitol standard.

3. Results and discussion

Scanning electron microscopy (SEM) was used to clarify the surface and shape characteristics of the particles. Electron microscopy observations showed a hollow surface that confirms the existence of hundreds of smaller crystallites inside every particle. The shape is different depending on the recrystallization method used (Fig. 1). The recrystallized forms obtained by the spray-drying presented a smooth and spherical appearance, whereas the rotary evaporation presented a sharp and acicular appearance.

Differential scanning calorimetry (DSC) technique may be used to confirm the existence of different polymorphs and pseudopolymorphs (solvates) (Otsuka et al., 1993; Shively and Myers, 1993; Grocker and McCauley, 1995; Saleki-Gerhardt et al., 1995; Ward and Schultz, 1995). This technique may also be used to confirm the presence of thermodynamically stable forms in this temperature range (Jozwiakowski et al., 1996).

The DSC scans of the recrystallized forms I and II (Fig. 2) show two endotherms. The first endotherm (140–143°C) is due to the melting of ASA. The second endotherm (165–167°C) is due to the melting of mannitol. The existence of a single endothermic peak for the different ASA samples shows that it is the thermodynamically stable form in this temperature range.

None of the samples showed any significant thermal event. The lower melting point observed in the recrystallized samples (methods I and II) as compared with the non-recrystallized forms may be attributed to variations in crystallinity.

The molecular states of ASA and mannitol molecules in I and II recrystallized forms were studied by means of infra-red spectroscopy. Fig. 3 shows the infra-red (IR) spectrum of ASA in the range of 500–4000 cm^{-1} . The spectrum of ASA crystals was characterized by the acetoxyl and carboxyl carbonyl stretching bands at 1753.6 and 1689.8 cm^{-1} , respectively. The spectrum of man-

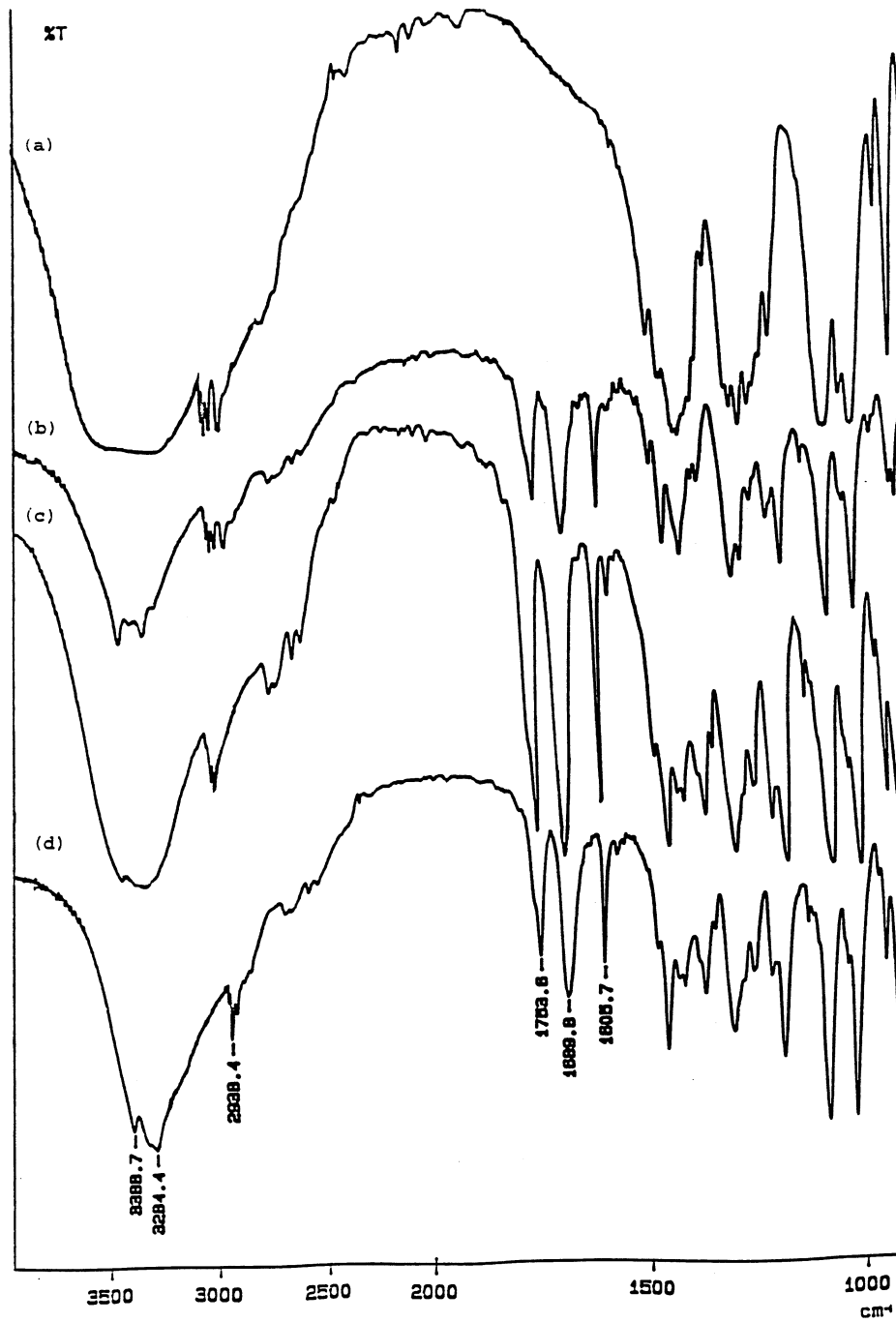


Fig. 3. Infra-red spectroscopy (FT-IR) of: (a) mannitol standard; (b) ASA standard; (c) spray-drier recrystallized form I-(3:1); and (d) rotary recrystallized form II-(3:1).

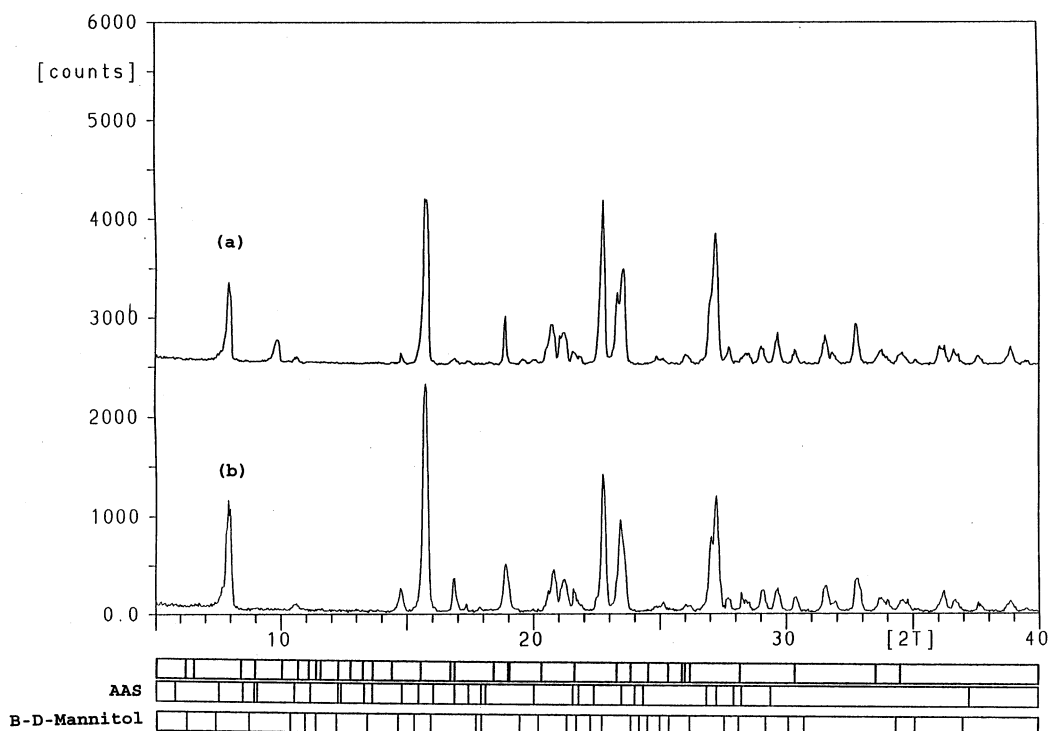


Fig. 4. Powder X-ray diffraction scans of the two crystalline forms that coexist in (a) the spray-drier recrystallized sample I(3:1) and (b) the rotary evaporation recrystallized sample II(3:1) versus the diffraction patterns collected in ASCIT tables for ASA (CAS:50-78-2) and mannitol (CAS:69-65-8).

nitrol crystals was characterized by the hydroxyl stretching bands in $3400\text{--}3200\text{ cm}^{-1}$ range. The IR spectra of the forms I and II were found to be similar to those of the ASA crystal standard sample (physical mixture ASA:mannitol 4:0) without changes in monomeric ASA molecules caused by these recrystallization methods.

The X-ray powder diffraction (Fig. 4) shows that none of the different recrystallization methods used produces a displacement on the diffraction patterns of the two crystalline forms that coexist in the different samples, and both present similar diffraction patterns to those collected in ASCIT tables for ASA (monoclinic crystal, CAS: 50-78-2) and mannitol (orthorhombic crystal, CAS: 69-65-8).

These results show that there are no ASA disordered structures when different mannitol ratios are employed in the recrystallization methods. However, with some polymers such as β -cy-

clodextrin, crystalline structural changes were observed during the recrystallization process (Oguchi et al., 1990; Connolly et al., 1996; Torrado et al., 1996b).

The average crystallite sizes were evaluated by means of Scherrer's equation. The instrumental broadening was determined using an ASA standard which has a crystallite size bigger than $1\text{ }\mu\text{m}$. The standard was considered acceptable as its full widths at half maximum (FWHM) for the two peaks at 7.891° and 15.857° (2θ) presented similar values of 0.174 and 0.171 respectively, which led us to suppose that the standard width corresponds to the instrumental broadening.

Table 1 shows the crystallite size and mean dissolution time in vitro ($\text{MDT}^{\text{vitro}}$) of the different recrystallized forms. For both recrystallization methods a great decrease in the ASA crystal size ($1150\text{--}1950\text{ \AA}$) was observed as compared with the standard ASA ($>10000\text{ \AA}$). Moreover, the

Table 1

Powder X-ray diffraction parameters: peak breadth, intensity and ASA crystallite size and mean dissolution time in vitro (MDT^{vitro}) of the different recrystallized forms

Samples	Peak breadth	Intensity	ASA crystallite size (Å)	MDT ^{vitro} (min)
Standard ASA	0.166	22764	> 10 000	12.92
Method I (ASA:mannitol)				
I-(4:0)	0.213	2077	1678	5.01
I-(3:1)	0.219	316	1832	5.09
I-(1:1)	0.211	452	1532	4.98
I-(1:3)	0.219	274	1926	3.18
Method II (ASA:mannitol)				
II-(4:0)	0.231	2515	1180	4.79
II-(3:1)	0.191	1744	1147	4.08
II-(1:1)	0.232	525	1201	3.06
II-(1:3)	0.236	303	1405	6.06

spray-dried recrystallized forms presented slightly higher values of crystallite size than the rotary evaporation samples independent of the ASA:mannitol ratios assayed. Thus, the results show that there is not a clear relationship between the ASA:mannitol ratio and the ASA crystallite size of recrystallized forms.

The physical mixtures of ASA and mannitol at various ratios (4:0, 3:1, 1:1 and 1:3) let us evaluate the influence of mannitol in the dissolution profile of ASA. Fig. 5 shows the dissolution curves of these physical mixtures. The simple addition of mannitol to the drug in a physical mixture does not increase the ASA dissolution rate.

During the recrystallization processes it was observed that all the recrystallized forms presented lower bulk density than the respective physical mixtures. The I-(1:3) recrystallized form presented the lowest bulk density.

However, the recrystallized forms obtained by either recrystallization method, presented a faster dissolution rate than the physical mixture with the same ASA:mannitol ratio (Table 1 and Figs. 5–7), which can be explained, in large measure, by the great reduction of the ASA crystallite size obtained with both recrystallization methods (Table 1) as compared with the standard ASA crystallite size.

The release profile of the spray-dried recrystallized form I-(1:3) was faster than the other recrystallized

tallized samples obtained by the same method (Fig. 6). This result may be explained by the fact that this recrystallized form I-(1:3) presented the smallest bulk density.

Of the recrystallized forms obtained by rotary evaporation the faster dissolution rates were obtained with the ASA:mannitol ratios of 3:1 and 1:1, while with a higher proportion of mannitol (formulation II-(1:3)), a clear decrease in the dissolution rate was observed (Fig. 7). All these rotary recrystallized forms presented similar values of bulk density. The slowest dissolution rate observed for the formulation II-(1:3) may be attributed to its bigger crystal size.

As there are no changes in the ASA chemical structure studied by infra-red spectroscopy (FT-IR), the different dissolution profiles must be due to changes in the crystallinity percentage or to changes in the crystallite size generated during the recrystallization process.

In summary, small differences in microcrystallinity in recrystallized forms can be difficult to detect. Only by using a variety of analytical methods can the elucidation of differences in powder crystallinity be fully ascertained. Scanning electron microscopy was applied for detecting changes in particle morphology. Differential scanning calorimetry (DSC) technique was used to rule out the existence of different polymorphs and

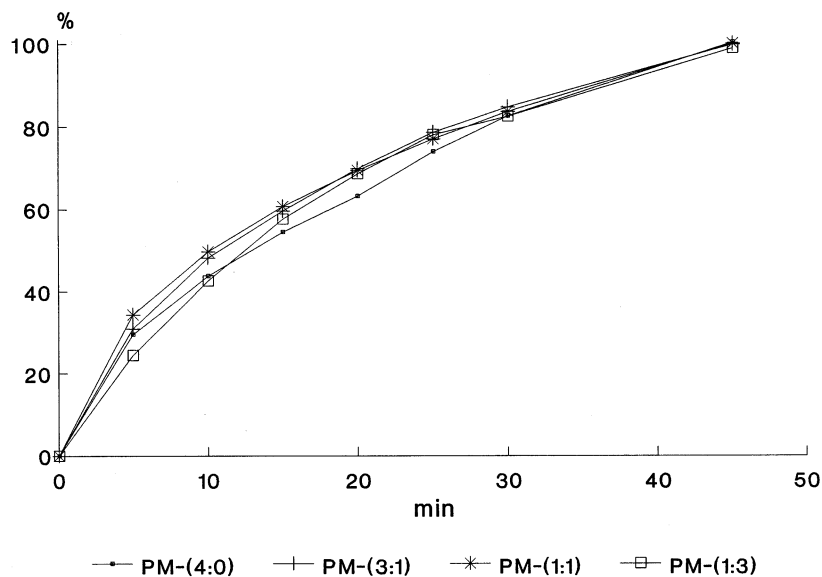


Fig. 5. Dissolution profiles of the physical mixtures (PM) of ASA:mannitol at different ratios 4:0 (small open box on line), 3:1 (vertical mark through line), 1:1 (asterisk on line) and 1:3 (large open box on line).

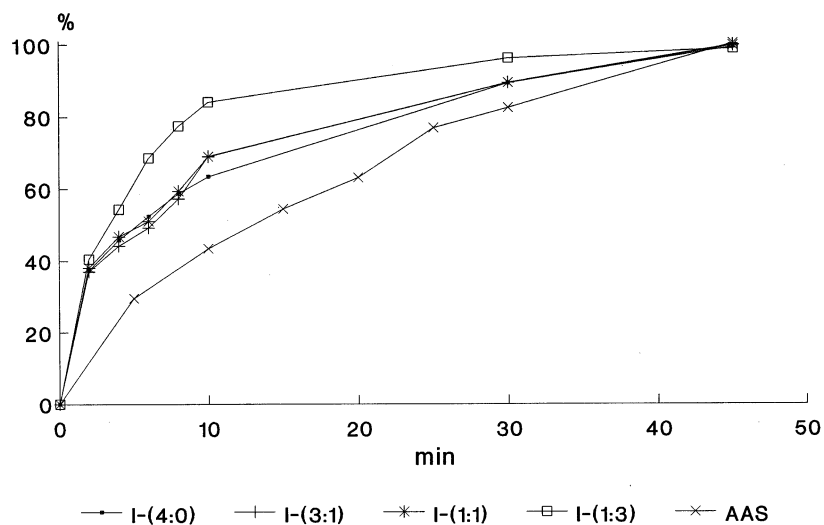


Fig. 6. Dissolution profiles of the spray-dried recrystallized forms (method I) of ASA:mannitol at different ratios 4:0 (small open box on line), 3:1 (vertical mark through line), 1:1 (asterisk on line), 1:3 (large open box on line) and non-recrystallized standard ASA (cross on line).

pseudopolymorphs (solvate) or totally amorphous forms. Infra-red spectroscopy provides information about possible chemical structural changes. Powder X-ray diffraction was used to obtain the microcrystallite size.

We can thus conclude that both recrystallization methods achieve a great reduction of the ASA crystallite size which could explain the faster dissolution rate of the recrystallized samples as compared to physical mixtures.

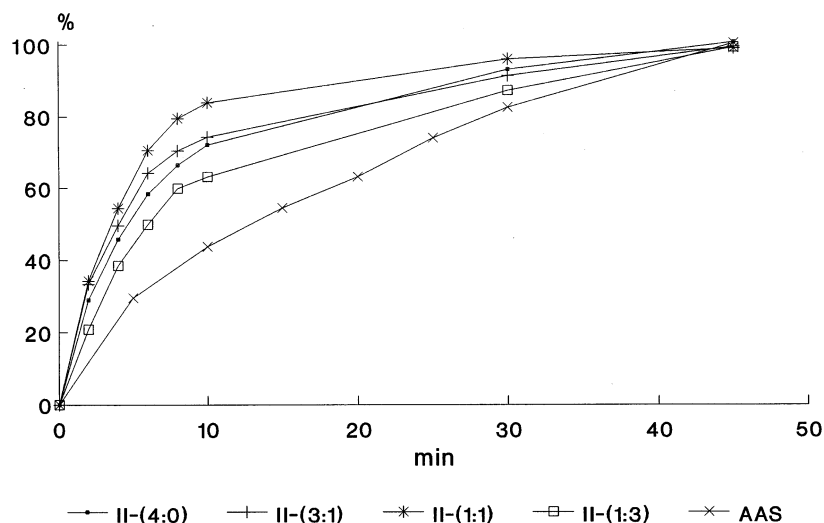


Fig. 7. Dissolution profiles of the rotary evaporated recrystallized forms (method II) of ASA:mannitol at different ratios 4:0, 3:1 (small open box on line), 1:1 (vertical mark on line), 1:3 (asterisk on line) and non-recrystallized standard ASA (cross on line).

References

- Buckton, G., Choularton, A., Beezer, A., Chatham, S., 1988. The effect of the comminution technique on the surface energy of a powder. *Int. J. Pharm.* 47, 121–128.
- Caira, M.R., Easter, B., Honiball, S., Horne, A., Nassimbeni, L.R., 1995. Structure and thermal stability of alprazolam and selected solvates. *J. Pharm. Sci.* 84, 1379–1384.
- Connolly, M., Debenedetti, P.G., Tung, H., 1996. Freeze crystallization of imipenem. *J. Pharm. Sci.* 85, 174–177.
- Duddu, S.P., Weller, K., 1996. Importance of glass transition temperature in accelerated stability testing of amorphous solid: case study using a lyophilized aspirin formulation. *J. Pharm. Sci.* 85, 345–347.
- Ghosh, S., Ojala, W.H., Gleason, W.B., Grant, D.J.W., 1995. Relationships between crystal structures, thermal properties and solvate stability of dialkylhydroxypyridones and their formic acid solvates. *J. Pharm. Sci.* 84, 1392–1399.
- Grocker, L.S., McCauley, J.A., 1995. Comparison of the crystallinity of imipenem samples by X-ray diffraction of amorphous material. *J. Pharm. Sci.* 84, 226–227.
- Jozwiakowski, M.J., Ngugen, N.T., Sisco, J.M., Spancake, C.W., 1996. Solubility behavior of lamivudine crystal forms in recrystallization solvents. *J. Pharm. Sci.* 85, 193–199.
- Oguchi, T., Okada, M., Yonemochi, E., Yamamoto, K., Nakai, Y., 1990. Freeze-drying of drug-additive binary systems III. Crystallization of alfa-cyclodextrin inclusion complex in freezing process. *Int. J. Pharm.* 61, 27–34.
- Otsuka, M., Onoe, M., Matsuda, Y., 1993. Physicochemical stability of phenobarbital polymorphs at various levels of humidity and temperature. *Pharm. Res.* 10, 577–582.
- Saleki-Gerhardt, A., Stowell, J.G., Byrn, S.R., Zografi, G., 1995. Hydration and dehydration of crystalline and amorphous forms of raffinose. *J. Pharm. Sci.* 84, 318–322.
- Schreiner, W.N., Jenkins, R., 1983. Profile fitting for quantitative analysis in X-ray powder diffraction. *Adv. X-Ray Anal.* 26, 141–148.
- Shively, M.L., Myers, S., 1993. Solid-state Emulsions: the effects of process and storage conditions. *Pharm. Res.* 10, 1071–1075.
- Torrado, S., Cadórniga, R., Torrado, J.J., 1996a. Effect of drug release rate on bioavailability of different aspirin tablets. *Int. J. Pharm.* 133, 65–70.
- Torrado, S., Torrado, S., Torrado, J.J., Cadórniga R., 1996b. Preparation dissolution and characterization of albendazole solid dispersions. *Int. J. Pharm.* 140, 247–250.
- Ward, G.H., Schultz, R.K., 1995. Process-induced crystallinity changes in albuterol sulfate and its effect on powder physical stability. *Pharm. Res.* 12, 773–779.